Inorg. Chem. **2008**, *47*, 10971−10979

Comparative Behavior of Britholites and Monazite/Brabantite Solid Solutions during Leaching Tests: A Combined Experimental and DFT Approach

E. Veilly,[†] E. du Fou de Kerdaniel,[*,†] J. Roques,[†] N. Dacheux,[†,‡] and N. Clavier[†,‡]

Groupe de Radiochimie, Institut de Physique Nucléaire d'Orsay, UMR 8608 CNRS/Université Paris-Sud-11, Bât. 100, Université Paris-Sud-11, 91406 Orsay Cedex, France and Institut de Chimie Séparative de Marcoule, UMR 5257 CNRS/CEA/UM2/ENSCM, Centre de Marcoule, BP 17171, 30207 Bagnols sur Cèze, France

Received June 24, 2008

In the field of the specific immobilization of actinides, several phosphate-based ceramics have already been proposed as suitable candidates. Among them, britholite and monazite/brabantite (now called monazite/cheralite) solid solutions have been considered as serious candidates on the basis of several properties of interest. Although both matrices appear almost similar from a chemical point of view, their chemical behavior during leaching tests appear to be strongly different with normalized dissolution rates of typically (2.1 ± 0.2) $g \cdot m^{-2} \cdot day^{-1}$ for Th-britholites (10^{-1}M HNO_3, θ = 25 °C, dynamic conditions) and (2.2 ± 0.2) 10^{-5} $g \cdot m^{-2} \cdot day^{-1}$ for Th-brabantites (10^{-1}M HNO_3, θ = 90 °C, dynamic conditions). To understand such difference from a crystallographic point of view, comparative leaching tests have been performed using either high or low renewal of the leachate. The results obtained clearly revealed a lower chemical durability of An-britholites compared to that of (Ln, Ca, An)-monazite/brabantite solid solutions. As a confirmation of this point, density functional theory calculations clearly showed some great differences in the cohesive energy of calcium in both crystal structures, which can explain this strong difference in the chemical durability of both materials.

1. Introduction

Phosphate-based ceramics such as monazites have already been described as potential candidates for the specific immobilization of long-life radionuclides, and especially actinides, coming from the back-end of the nuclear fuel cycle. Indeed, phosphate-based minerals often present high weight loadings in actinides (up to 15 wt % in ThO_2 or UO_2)[1,2] associated to strong resistances to aqueous corrosion and to radiation damages.[3,4] Such properties led the French Research Groups NOMADE then MATINEX (CNRS/CEA/AREVA/EDF/French Universities) to select then to study thoroughly four optimized matrices. Among them, three phosphate-based ceramics[5] were examined: thorium phosphate−diphosphate ($Th_4(PO_4)_4P_2O_7$, β-TPD)[6−12] with associated β-TPD/monazite compounds,[13] britholites ($Ca_9Ln_{1-x}An^{IV}_x(PO_4)_{5-x}$-

* To whom correspondence should be addressed. Phone: +33 4 66 90 57 65; Fax: + 33 4 66 33 92 05; E-mail: nicolas.dacheux@univ-montp2.fr, nicolas.dacheux@icsm.fr.
† Institut de Physique Nucléaire d'Orsay.
‡ Institut de Chimie Séparative de Marcoule.

(1) Boatner, L. A. *Rev. Mineral. Chem.* **2002**, *48*, 87–121.
(2) Ewing, R. C. *Progr. Nucl. Energy* **2007**, *49*, 635–643.
(3) Meldrum, A.; Boatner, L. A.; Weber, W. J.; Ewing, R. C. *Geochim. Cosmochim. Acta* **1998**, *62*, 2509–2520.
(4) Ewing, R. C.; Harker, R. F. *Nucl. Chem. Waste Manage.* **1980**, *1*, 51–57.
(5) Dacheux, N.; Clavier, N.; Robisson, A.C.; Terra, O.; Audubert, F.; Lartigue, J. E.; Guy, C. *C.R. Acad. Sc. Paris* **2004**, *7*, 1141–1152.
(6) Benard, P.; Brandel, V.; Dacheux, N.; Jaulmes, S.; Launay, S.; Lindecker, C.; Genet, M.; Louër, D.; Quarton, M. *Chem. Mater.* **1996**, *8*, 181–188.
(7) Dacheux, N.; Brandel, V.; Genet, M.; Bak, K.; Berthier, C.; New, J. *Chem.* **1996**, *20*, 301–310.
(8) Brandel, V.; Dacheux, N.; Genet, M. *J. All. Comp.* **1998**, *271−273*, 236–239.
(9) Dacheux, N.; Chassigneux, B.; Brandel, V.; Le Coustumer, P.; Genet, M.; Cizeron, G. *Chem. Mater.* **2002**, *14*, 2953–2961.
(10) Dacheux, N.; Podor, R.; Brandel, V.; Genet, M. *J. Nucl. Mater.* **1998**, *252*, 179–186.
(11) Dacheux, N.; Thomas, A. C.; Brandel, V.; Genet, M. *J. Nucl. Mater.* **1998**, *257*, 108–117.
(12) Robisson, A. C.; Dacheux, N.; Aupiais, J. *J. Nucl. Mater.* **2002**, *306*, 134–146.
(13) Clavier, N.; Dacheux, N.; Podor, R. *Inorg. Chem.* **2006**, *45*, 220–229.

10.1021/ic801169d CCC: $40.75
Published on Web 10/29/2008

$(SiO_4)_{1+x}F_2$),[14−17] and $Ln^{III}_{1-2x}Ca^{II}_xAn^{IV}_xPO_4$ monazites/brabantite solid solutions[18−25] (this latter being recently renamed as cheralite, according to the CNMMN nomenclature[26]).

Monazite ($M^{III}PO_4$, monoclinic system, $P2_1/n$, $Z = 4$) is reported to be the most abundant lanthanide ore on earth and represents the main thorium mineral source[27] with high thorium weight loadings.[28−30] In this structure, the incorporation of trivalent actinides occurs through the direct substitution of lanthanide atoms, whereas that of tetravalent elements is usually described by two coupled substitutions: $2\ Ln^{3+} \leftrightarrow (Th,U)^{4+} + Ca^{2+}$ (widely predominant) and $Ln^{3+} + PO_4^{3-} \leftrightarrow (Th,U)^{4+} + SiO_4^{4-}$. By the first way, ideal $Ln^{III}_{1-2x}Ca^{II}_xAn^{IV}_xPO_4$ solid solutions (noted (Ln, Ca, An) − Monazite/Brabantite or Monazite/Cheralite) were prepared in the $LaPO_4-Ca_{0.5}Th_{0.5}PO_4$[31] and $LaPO_4-Ca_{0.5}U_{0.5}PO_4$[32] binaries provided that the following inequalities are respected:[21]

$$1.107\ \text{Å} \leq \overline{{}^{IX}r_{M^{II+III+IV}}} \leq 1.216\ \text{Å and}$$

$$1 \leq \overline{{}^{IX}r_{M^{II+III}}}/\overline{{}^{IX}r_{M^{III+IV}}} \leq 1.238 \quad (1)$$

where

$$\overline{{}^{IX}r_{M^{II+III+IV}}} = (1-2x)\ {}^{IX}r_{M^{III}} + x\,{}^{IX}r_{M^{II}} + x\,{}^{IX}r_{M^{IV}} \quad (2)$$

and

$$\overline{{}^{IX}r_{M^{II+III}}}/\overline{{}^{IX}r_{M^{III+IV}}} = \frac{[(1-2x)\,{}^{IX}r_{M^{III}} + x\,{}^{IX}r_{M^{II}}]}{(1-2x)\,{}^{IX}r_{M^{III}} + x\,{}^{IX}r_{M^{IV}}} \quad (3)$$

A lot of methods, based either on wet (including hydrothermal conditions) or dry chemistry processes, are mentioned in the literature for the preparation of monazite, brabantite (cheralite), and/or monazite/brabantite (monazite/cheralite) solid solutions samples.[33−49] Several of these methods led to the incorporation of tri- and/or tetravalent actinides in the monazite structure. Moreover, some recent works were developed to improve the cation distribution thanks to the repetition of grinding/heating steps for $Ca_{0.5}Th_{0.5-y}U_yPO_4$ and $Ln_{1-2x}Ca_xTh_{x-y}U_yPO_4$ solid solutions.[21,50] From all these studies, it appeared difficult to incorporate plutonium or cerium in their tetravalent form.[20,21]

The incorporation of actinides in britholites of formula $Ca_9Ln_{1-x}An^{IV}_x(PO_4)_{5-x}(SiO_4)_{1+x}F_2$,[51,52] was mainly driven by geological considerations based on natural apatites (particularly those coming from the Oklo fossil nuclear reactors − Gabon). The precise characterization of such samples revealed that the britholite structure can accept a large variety of cationic substitutions, leading to the simultaneous incorporation of lanthanides, thorium, and uranium.[15,53] Some samples of silicate-based apatite (britholites) of In Ouzzal site (Algeria) were found to locally contain up to 50 wt % of actinides (U,Th).[54] Moreover, the apatite structure seems to be able to anneal the defects generated by self-irradiation even at low temperature.[55] However, the metamictization process (destruction of the crystal lattice due to radiation damage) strongly depends on the chemical composition of

(14) Carpena, J.; Audubert, F.; Bernache, D.; Boyer, L.; Donazzon, B.; Lacout, J. L.; Senamaud, N.; *Scientific Basis for Nuclear Waste Management XXI*, McKinley, I. G.; McCombie, C. Eds.; 1998; Vol. *506*, p 543.
(15) Bros, R.; Carpena, J.; Sere, V.; Beltritti, A. *Radiochim. Acta* **1996**, *74*, 277–282.
(16) Terra, O.; Audubert, F.; Dacheux, N.; Guy, C.; Podor, R. *J. Nucl. Mater.* **2007**, *366*, 70–86.
(17) Terra, O.; Audubert, F.; Dacheux, N.; Guy, C.; Podor, R. *J. Nucl. Mater.* **2006**, *354*, 49–65.
(18) Montel, J. M.; Devidal, J. L.; Avignant, D. *Chem. Geol.* **2002**, *191*, 89–104.
(19) Podor, R.; Cuney, M.; Nguyen Trung, C. *Am. Mineral.* **1995**, *80*, 1261–1268.
(20) Bregiroux, D.; Belin, R.; Valenza, P.; Audubert, F.; Bernache-Assollant, D. *J. Nucl. Mater.* **2007**, *366*, 52–57.
(21) Bregiroux, D.; Terra, O.; Audubert, F.; Dacheux, N.; Serin, V.; Podor, R.; Bernache-Assollant, D. *Inorg. Chem.* **2007**, *46*, 10372–10382.
(22) Terra, O.; Dacheux, N.; Audubert, F.; Podor, R. *J. Nucl. Mater.* **2006**, *352*, 224–232.
(23) Boatner, L. A.; Sales, B. C.; *Radioactive Waste Forms for the Future*, Lutze, W., Ewing, R. C. Eds.; North-Holland Physics Publishing: Amsterdam, 1998, p 495.
(24) Meldrum, A.; Boatner, L. A.; Weber, W. J.; Ewing, R. C. *Geochim. Cosmochim. Acta* **1998**, *62*, 2509–2520.
(25) Terra, O.; Clavier, N.; Dacheux, N.; Podor, R.; New, J. *Chem.* **2003**, *27*, 957–967.
(26) Linthout, K. *Can. Mineral.* **2007**, *45*, 503–508.
(27) Schapira, J. P.; Singhal, R. K. *Nucl. Technol.* **1999**, *128*, 25–34.
(28) Förster, H. J. *Am. Mineral.* **1998**, *83*, 259–272.
(29) Montel, J. M.; Kornprobst, J.; Vielzeuf, D. *J. Metamorph. Geol.* **2000**, *3*, 335–342.
(30) Förster, H. J.; Harlov, D. E. *Mineral. Mag.* **1999**, *63*, 587–594.
(31) Podor, R.; Cuney, M. *Am. Mineral.* **1997**, *82*, 765–771.
(32) Rose, D. *N. Jb. Miner. Mh.* **1980**, *H* (6), 247–257.
(33) Jonasson, R. G.; Vance, E. R. *Thermochim. Acta* **1986**, *108*, 65–72.
(34) Drozdzynski, J. *Inorg. Chim. Acta* **1979**, *32*, L83–L85.
(35) Cleveland, J. M.; *The Chemistry of Plutonium*; Gordon & Breach Science Publishers: New-York, 1970.
(36) Bjorklund, C. W. *J. Am. Chem. Soc.* **1957**, *79*, 6347–6350.
(37) Aloy, A. S.; Kovarskaya, E. N.; Koltsova, T. I.; Samoylov, S. E.; *Radioactive Waste Management and Environmental Remediation*; ASME: 2001.
(38) Weigel, F.; Haug, H. *Radiochim. Acta* **1965**, *4*, 227–228.
(39) Hobart, D. E.; Begun, G. M.; Haire, R. G.; Hellwege, H. E. *J. Raman Spectrosc.* **1983**, *14*, 59–62.
(40) Muto, T.; Merowitz, R.; Pommer, A. M.; Murano, T. *J. Am. Mineral.* **1959**, *44*, 633–650.
(41) Feigelson, R. S. *J. Am. Ceram. Soc.* **1964**, *47*, 257–258.
(42) Kelly, K. L.; Beall, G. W.; Young, J. P.; Boatner, L. A.; *Scientific Basis for Nuclear Waste Management*, Moore, J. G. Ed.; New York, 1981; Vol. *3*, p 189.
(43) Boatner, L. A.; Beall, G. W.; Abraham, M. M.; Finch, C. B.; Hurray, P. G.; Rappaz, M.; *Scientific Basis for Nuclear Waste Management*, Northrup C. J. M., Jr. Ed.; New York, 1980; Vol. *2*, p 289.
(44) Mullica, D. F.; Sappenfield, E. L.; Wilson, G. A. *Lanthanide Actinide Res.* **1989**, *3*, 51.
(45) Montel, J. M.; Devidal, J. L.; *EUG XI, Symposium PCM6*, Strasbourg, France, April 8−12, 2001; Cambridge Publication: 2001; p 680.
(46) Pepin, G. J.; Vance, E. R.; McCarthy, G. J. *Mater. Res. Bull.* **1981**, *16*, 627–633.
(47) Tabuteau, A.; Pagès, M.; Livet, J.; Musikas, C. *J. Mat. Sc. Let.* **1988**, *7*, 1315–1317.
(48) Seaborg, G. T.; *Plutonium Chemistry*, Carnall, W. T., Choppin, G. R. Eds.; American Chemical Society: Washington DC, 1983.
(49) Bamberger, C. E.; Haire, R. G.; Hellwege, H. E.; Begun, G. M. *J. Less Common Metals* **1984**, *97*, 349–356.
(50) Terra, O.; Dacheux, N.; Clavier, N.; Podor, R.; Audubert, F. *J. Am. Ceram. Soc.* **2008**, doi: 10.1111/j.1551−2916.2008.02678.x.
(51) Boyer, L.; Savariault, J. M.; Carpéna, J.; Lacout, J. L. *Acta Crystallogr.* **1998**, *C54*, 1057–1059.
(52) Boyer, L.; *Synthèses et Caractérisations d'Apatites Phospho-silicatées aux Terres Rares: Application au Nucléaire*, PhD Thesis, INP Toulouse, 1998.
(53) Sère, V.; *Géochimie des minéraux néoformés à Oklo (Gabon), histoire géologique du bassin d'Oklo: une contribution pour les études de stockages géologiques de déchets radioactifs*, PhD Thesis, University of Paris VII, 1996.
(54) Carpéna, J.; Kienast, J. R.; Ouzegane, K.; Jehanno, C. *Geol. Soc. Amer. Bull.* **1988**, *100*, 1237–1243.
(55) Carpéna, J.; *Advances in Fission Track Geochronology*, Van den Haute, P., de Corte, F. Eds.; Kluwer Academie Press: 1998; p 81.

the apatites[55,56] and led to consideration of the monosilicated britholite $Ca_9Nd(PO_4)_5(SiO_4)F_2$ as the starting material.[51,52,57]

On the basis of these results, the incorporation of thorium in synthetic britholite samples was first examined to prepare fully silicated apatite $Ca_6Th_4(SiO_4)_6O_2$[58] then, more recently, $Ca_9Nd_{1-x}Th_x(PO_4)_{5-x}(SiO_4)_{1+x}F_2$ solids ((Nd,Th)-britholites) through the coupled substitution (Nd^{3+}, PO_4^{3-}) ⇔ (Th^{4+}, SiO_4^{4-}).[17,22] For the latter, the use of successive mechanical grinding steps (15 min, 30 Hz) allowed an increase in the specific surface area (thus the reactivity) of the mixture and led to a better homogeneity of the final samples. By this way, powdered and sintered samples of (Nd,Th)-britholites were prepared as pure and single phase compounds.[22]

In the same way, several attempts to incorporate uranium in britholites from both stable oxidation states U(VI) and U(IV) were reported in the literature during the last years.[59−62] More recently, a systematic study was devoted to the preparation of $Ca_9Nd_{1-x}U_x(PO_4)_{5-x}(SiO_4)_{1+x}F_2$ ((Nd,U)-britholites) samples.[16] Although the thorium incorporation is easy and quantitative in the britholite structure, that of tetravalent uranium is complicated by its redox properties. Indeed, all the final samples prepared at 1400 °C were found to be composed of $Ca_9Nd_{1-x}U_x(PO_4)_{5-x}(SiO_4)_{1+x}F_2$ and calcium uranate CaU_2O_{5+y}, which results from the formation of $CaUO_4$ above 800 °C consequently to the direct reaction between UO_2 and CaO.[16] The uranium incorporation was thus improved using two main methods: compaction of the powdered initial mixture prior to the heating treatment at 1400 °C or simultaneous incorporation of thorium and uranium in their tetravalent forms.[16,22]

As it was stated previously, the synthesis and then sintering of homogeneous and single-phase compounds of both phosphate-based materials families were already reported in several papers. Conversely, the literature dealing with the chemical durability of (Ln,Ca,An)-monazite/brabantites and (Nd,An)-britholites during leaching/dissolution processes, especially through the description of the associated successive chemical steps, remains rather poor. Only few results related to the chemical durability of synthetic monazite/brabantite solid solutions are reported in literature. Leaching tests performed in distilled water at 200 °C on $LaPO_4$ samples containing americium (up to 0.5 wt %) revealed a higher chemical durability than borosilicate glasses.[63] More recently, the dissolution of natural monazite was reported by Oelkers *et al.* as a function of temperature (50−230 °C) and pH (1−10). This study led to normalized dissolution rates between 8×10^{-7} g·m^{-2}·day^{-1} and 6×10^{-4} g·m^{-2}·day^{-1} at 70 °C.[64] A complementary study developed by Poitrasson et al. underlined the significant role of the solubility-controlling phases (such as $NdPO_4 \cdot {}^1/_2\ H_2O$) formed near to thermodynamic equilibrium, which rapidly ensure the efficient immobilization of trivalent lanthanides (and thus also actinides).[65]

The study of the chemical durability of britholite samples was mainly driven on natural samples.[5] However, some data are available on Nd-britholite samples for several temperatures (25−100 °C) and pH values. From this study, the dissolution was clearly incongruent due to the preferential release of several elements such as calcium or fluor in the leachate. For leaching tests with high renewal of the solution, the normalized dissolution rate determined from the calcium release was evaluated to 10^{-2} g·m^{-2}·day^{-1} at pH = 5.7 and T = 90 °C.[66] On the basis of the release of the other elements, normalized dissolution rates were also determined at pH = 4 ($R_L \approx 2 \times 10^{-3}$ g·m^{-2}·day^{-1}) and pH = 7 ($R_L \approx 5 \times 10^{-1}$ g·m^{-2}·day^{-1}).[5,67] Finally, when leaching the samples in the conditions of low-renewal of the leachate, the precipitation of Nd-rhabdophane (i.e., $NdPO_4 \cdot {}^1/_2\ H_2O$) already reported for monazite/brabantite (monazite/cheralite) samples was clearly evidenced.[5,68,76]

Considering the scarce literature dealing with the resistance of An-bearing britholites and monazite/brabantite (monazite/cheralite) solid solutions to aqueous corrosion, comparative leaching experiments were simultaneously conducted on both kinds of materials in several acidic media. The results obtained during such leaching tests were analyzed in the light of periodic density functional theory (DFT) calculations to explain the differences observed from structural and energetic points of view.

2. Methods

2.1. Samples Preparation. As already discussed, actinides-bearing britholites and monazite/brabantite (monazite/cheralite) solid solutions were prepared through the dry chemistry process already described in our published work.[16,17,22,50] In this field, powdered oxides (AnO_2, CaO, SiO_2), dicalcium diphosphate ($Ca_2P_2O_7$), and calcium difluoride (CaF_2) were mechanically ground and then fired at high temperature (T = 800 °C and t = 8 h for monazite/brabantite solid solutions or T = 1390 °C and t = 6 h for britholites). The resulting powder was again mechanically ground and then pressed in a tungsten carbide die (200−800 MPa). The cylindrical pellets were then fired once again at 1390 °C for 6 h for britholites and at 1300 °C for 10 h for monazite/brabantite solid solutions.

(56) Soulet, S.; Carpéna, J.; Chaumont, J.; Krupa, J. C.; Ruault, M. O. *J. Nucl. Mater.* **2001**, *299*, 227.
(57) Audubert, F.; Bernache-Assolant, D.; *Advances in Science and Technology − Proceedings of the 10th International Ceramics Congress-CIMTEC 2002*, Faenza, Italy, 2002; Vincenzini, P. Ed.; 2002; vol. *31*, Part B, p 61.
(58) Engel, G. *Mater. Res. Bull.* **1978**, *13*, 43–48.
(59) Rakovan, J.; Reeder, R. J.; Elzinga, E. J.; Cherniak, D. J.; Tait, C. D.; Morris, D. E. *Environ. Sci. Technol.* **2002**, *36*, 3114–3117.
(60) Vance, E. R.; Carter, M. L.; Begg, B. D.; Day, R. A.; Leung, S. H. F. *Mater. Res. Soc. Symp. Proc.* **2000**, *608*, 431.
(61) Vance, E. R.; Ball, C. J.; Begg, B. D.; Carter, M. L.; Day, R. A.; Thorogood, G. J. *J. Am. Ceram. Soc.* **2003**, *86*, 1223–1225.
(62) El Ouenzerfi, R.; Cohen Adad, M. T.; Goutardier, C.; Panczer, G. *Solid State Ionics* **2004**, *176*, 225.
(63) Boatner, L. A.; Beall, G. W.; Abraham, M. M.; Finch, C. B.; Murray, P. G.; Rappaz, M.; *Scientific Basis for Nuclear Waste Management*, Northrup J. R., C.J.M. Eds.; New York, 1980; Vol. *2*, p. 289.
(64) Oelkers, E.; Poitrasson, F. *Chem. Geol.* **2002**, *191*, 73–87.
(65) Poitrasson, F.; Oelkers, E.; Schott, J.; Montel, J. M. *Geochim. Cosmochim. Acta* **2004**, *68*, 2207–2221.
(66) Guy, C.; Audubert, F.; Lartigue, J. E.; Latrille, C.; Advocat, T.; Fillet, C. *C.R. Phys.* **2002**, *3*, 827–837.
(67) Chaïrat, C.; Oelkers, E.; Köhler, S.; Harouiya, N.; *Water−Rock Interaction*, Wanty, R. B.; Seal, R. R. Eds.; 2004.
(68) Chaïrat, C.; Oelkers, E.; Schott, J.; Lartigue, J. E. *J. Nucl. Mater.* **2006**, *354*, 14–27.

2.2. Leaching Tests Procedure. Due to the strong resistance of the materials to alteration processes, leaching experiments were usually performed in several acidic media in order to increase the normalized dissolution rates and to describe more precisely the associated dissolution mechanisms.

Polytetrafluoroethylene (PTFE) containers were used in both low (static) and high (dynamic) renewal conditions. The samples (100−300 mg) were put in contact with 5−25 mL of solution. At regular intervals, the leachate was partly removed and then analyzed in order to determine the concentrations of the elements released in the leachate. In the case of static conditions, only 1−2% of the leachate was renewed by fresh solution. This slow leaching flow (around 10^{-1} mL·day^{-1}) allowed the consideration that the system was not modified by this uptake.

Unfortunately, for several compounds, static experiments usually led to the rapid saturation of the leachate, which can induce some discrepancies in the accurate determination of the normalized dissolution rates. To avoid/minimize such phenomena, dynamic experiments were also developed. The experiments took place in open PTFE reactors set in aluminum baths for temperatures ranging from 25 to 90 °C. The leaching solution was then injected into the reactor with a flow rate ranging from 2 to 40 mL·hour^{-1} through a 10 μm filter using a peristaltic pump.

For both leaching methods, the aliquotes were centrifugated at 4000 rpm and then finally at 13 000 rpm in order to avoid the eventual presence of colloids in the analyzed solutions.

The elementary concentrations were determined by ICP-AES (inductively coupled plasma-atomic emission spectroscopy) (Jobin Yvon Ultima) or KPA (kinetic phosphorescence analysis) for uranium (ChemChek Instruments, Richland, USA). For ICP-MS experiments, 1 ppb of terbium and bismuth were added to the samples as internal standards.

To avoid the initial artifact usually associated to the presence of minor and/or nonstoichiometric phases at the surface of the unwashed minerals, the samples were first washed with leaching solutions for 1−7 days at room temperature. This method allowed the elimination of the important increase of the concentration observed at the beginning of the dissolution curves.

Moreover, to get an accurate comparison of the various materials studied, the leachability of the element i is usually described by its normalized leaching, $N_L(i)$ (g·m^{-2}), which is defined by the relation:

$$N_L(i) = \frac{m_i}{f_i S} \tag{4}$$

where m_i corresponds to the total amount of i measured in the solution (g), S is the corresponding solid area (m^2) in contact with the solution, and f_i is the mass ratio of the element i in the solid.

The expression of the normalized dissolution rate, $R_L(i)$ (expressed in g·m^{-2}·day^{-1} and usually noted R_H in acidic media), can be deduced from the evolution of the normalized leaching, as follows:

$$R_L(i) = \frac{1}{f_i S} \times \frac{dm_i}{dt} = \frac{dN_L(i)}{dt} \tag{5}$$

By this way, the chemical durability of the samples is normalized by the reactive surface of solid in contact with the solution and by the elementary weight loading. When the dissolution occurs far from the equilibrium, the normalized dissolution rate is usually found to be constant.[69] On the contrary, near the equilibrium, saturation processes associated to the precipitation of neoformed phases onto the surface of the solids are usually involved.[70,78] The formation of such phases is often associated to the decrease of the normalized dissolution rates due to the diffusion of the leachable elements through the alteration layers.

2.3. Computational Details. Since the studied materials revealed strong differences during the leaching tests, periodic DFT calculations were performed using plane waves basis sets in order to determine the cohesive energy of calcium in (La,Ca,Th)-monazite/brabantite (monazite/cheralite) solid solutions and in (Nd,Th)-britholites. Calculations were carried out with the VASP (Vienna Ab Initio Simulation Package) code[71,72] using the Projector-Augmented-Wave (PAW) pseudopotentials for core-valence interactions.[73] Valence shells were $3p^64s^2$ for Ca atoms, $2s^22p^5$ for F atoms, $5p^66s^25d^1$ for La atoms, $5s^25p^66s^24f^1$ for Nd atoms, $2s^22p^4$ for O atoms, $3s^23p^3$ for P atoms, $3s^23p^2$ for Si atoms, and $6p^67s^26d^2$ for Th atoms. The wave functions were extended up to 300 eV for (La,Ca,Th)-monazite/brabantites and up to 330 eV for (Nd,Th)-britholites. The generalized gradient approximation (GGA) of Perdew−Wang (PW91)[74] was used to determine the exchange-correlation energy. All geometries and energies of the models were computed with (4 × 2 × 2) and (3 × 3 × 2) Monkhorst−Pack[75] sampling (centered at the Γ-point) in the Brillouin zone for (Nd,Th)-britholite and (La,Ca,Th)-monazite/brabantite, respectively. The convergence criterions for the self-consistency cycle and the maximum force were set at 10^{-4} eV and 0.002 eV·Å^{-1}, respectively. The lattice parameters were determined by relaxing the cell volume as well as the atomic positions.

3. Results and Discussion

3.1. Experimental Study of the Dissolution of Britholite Samples. As already mentioned, samples of $Ca_9Nd_{0.5}Th_{0.5}(PO_4)_{4.5}(SiO_4)_{1.5}F_2$ ((Nd,Th)-britholite) and $Ca_9Nd_{0.5}Th_{0.25}U_{0.25}(PO_4)_{4.5}(SiO_2)_{1.5}F_2$ ((Nd,Th,U)-britholites) were leached in static and dynamic conditions. In static conditions, the rapid saturation of the leachate observed whatever the experimental conditions led to some difficulties

(69) Dacheux, N.; Clavier, N.; Ritt, J. *J. Nucl. Mater.* **2006**, *349*, 291–303.
(70) Tamain, C.; Dacheux, N.; Garrido, F.; Thome, L. *J. Nucl. Mater.* **2007**, *362*, 459–465.
(71) Kresse, G.; Hafner, J. *J. Phys. Rev. B* **1993**, *47*, 558–561.
(72) Kresse, G.; Furthmüller, J. *J. Comput. Mater. Sci.* **1996**, *6*, 15–50.
(73) Kresse, G.; Joubert, D. *Physical Review B* **1999**, *59*, 1758–1775.
(74) Perdew, J. P.; Wang, Y. *Physical Review B* **1992**, *45*, 13244.
(75) Monkhorst, H. J.; Pack, J. D. *Physical Review B* **1976**, *13*, 5188–5191.
(76) Du Fou De Kerdaniel, E.; Clavier, N.; Dacheux, N.; Terra, O.; Podor, R. *J. Nucl. Mater.* **2007**, *362*, 451–458.

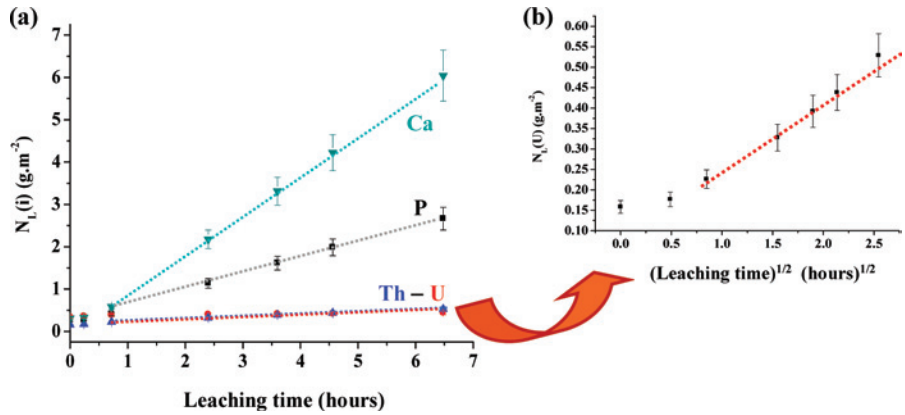

Figure 1. Evolution of N_L(Ca) (▼), N_L(P) (■), N_L(Th) (▲), and N_L(U) (●) during the dissolution of (Nd,Th,U)-britholites leached in 10^{-1}M HNO_3 at 90 °C (a) and associated variation of N_L(U) vs the square root of time (b).

in the determination of the normalized leaching rates. Indeed, the precipitation of thorium, calcium, and neodymium as a neoformed phase at the surface of the sample was correlated to the decrease of the uranium leaching rate, probably due to diffusion (or saturation) phenomena occurring at the solid/liquid interface. The chemical composition of such neoformed phase (EPMA results: 12.9 wt % (Nd), 1.5 wt % (Ca), 48.2 wt % (Nd), and 10.6 wt % (Th)) led to (Nd + Ca + Th)/P mole ratio close to 1,[76] which was identified to be hydrated (Ca,Nd,Th)-phosphate[76] with the rhabdophane structure.[77] From SEM, grazing XRD, and μ-Raman experiments, needle-like crystals of $Ca_xNd_{1-2x}Th_xPO_4 \cdot {}^1/_2\ H_2O$ rhabdophane (5−10 μm in length) were initially scarcely precipitated at the leached surface and then fully cover the entire surface for longer leaching times.[76]

Consequently, several leaching tests were also developed in dynamic conditions in order to move the system away from such thermodynamic equilibria and to avoid/minimize the associated described saturation processes. Such leaching tests were then undertaken on both (Nd,Th)-britholites and (Nd,Th,U)-britholites in several operating conditions (pH, temperature, etc.). Contrarily to the other elements, the thorium concentration was not determined with a good accuracy for the major part of the solids considered. For instance, the normalized dissolution rates determined when leaching (Nd,Th)-britholites samples at 25 °C in 10^{-1}M HNO_3 were evaluated to $R_L(Ca) \approx 2.1 \pm 0.2$ g·m^{-2}·day^{-1} and $R_L(P) \approx 0.7 \pm 0.1$ g·m^{-2}·day^{-1}. They revealed that the dissolution was clearly incongruent: the $R_L(Ca)/R_L(P)$ ratio being almost constant and higher than 3 (e.g., 3.1 for experiments performed in 10^{-1}M HNO_3 at room temperature). Moreover, they were found to be higher than that reported by Clavier et al. for sintered β-TUPD solid solutions[78] or β-TUPD/monazite samples.[13]

The influence of temperature was also clearly demonstrated. Indeed, the R_L(Ca) values increased from 2.6 ± 0.3 g·m^{-2}·day^{-1} at 50 °C to 10.3 ± 0.8 g·m^{-2}·day^{-1} at 90 °C, and that of R_L(P) increased from 0.9 ± 0.1 g·m^{-2}·day^{-1} to 3.2 ± 0.3 g·m^{-2}·day^{-1}. From all these data, the associated apparent activation energy values were evaluated to E_A = 34 ± 5 kJ·mol^{-1} and 31 ± 4 kJ·mol^{-1} considering the release of calcium and phosphorus, respectively. Both low values confirm the important role of surface reactions occurring at the solid/liquid interface.[79] Some additional experiments showing the influence of the medium acidity and of the concentration of strong complexing reagents (such as sulfate ions) regarding to tri- and tetravalent actinides on the normalized leaching rate will be reported in a forthcoming publication.

Table 1. Normalized Dissolution Rates Obtained When Leaching (Nd,Th,U)-Britholites in 10^{-1}M HNO_3 at 90°C

	R_L (i) (g·m^{-2}·day^{-1})			
time	Ca	P	Th	U
t <2 h	21.6 ± 2.0	9.1 ± 1.0	1.4 ± 0.1	2.3 ± 0.3
t > 2 h			0.23 ± 0.01	1.3 ± 0.2

On the basis of the results obtained for Th-britholites, several dissolution tests were also realized in 10^{-1}M HNO_3 at 90 °C on (Nd,Th,U)-britholites. The corresponding evolutions of the normalized leachings N_L(Ca), N_L(P), N_L(Th), and N_L(U) obtained with high renewal of the leachate (40 mL·h^{-1}) are reported in Figure 1. Once again, the dissolution of the material appears to be clearly and rapidly incongruent with the precipitation of thorium in neoformed phases after only 2 h of leaching time. The associated normalized dissolution rates (Table 1), which range from 0.23 ± 0.10 g·m^{-2}·day^{-1} (R_L(Th)) to 21.6 ± 2.0 g·m^{-2}·day^{-1} (R_L(Ca)), appear to be higher than those obtained during the dissolution of (Nd,Th)-britholites due to the presence of uranium in the samples. The chemical durability of britholite samples seems thus to be degraded consequently to the presence of the easily oxidized uranium in the prepared samples.

A significant decrease of the normalized dissolution rate R_L(U) is observed after 2 h of leaching time (Table 1). The linear variation of R_L(U) versus the square root of leaching time allows us to conclude that uranium is submitted to diffusion phenomena through the neoformed thorium-enriched alteration layer (Figure 1).

(77) Hezel, A.; Ross, S. D. *J. Inorg. Nucl. Chem.* **1967**, *29*, 2085–2089.
(78) Clavier, N.; Du Fou de Kerdaniel, E.; Dacheux, N.; Le Coustumer, P.; Drot, R.; Ravaux, J.; Simoni, E. *J. Nucl. Mater.* **2006**, *349*, 304–316.
(79) Lasaga, A. C. *Rev. Mineral.* **1981**, *8*, 135–169.

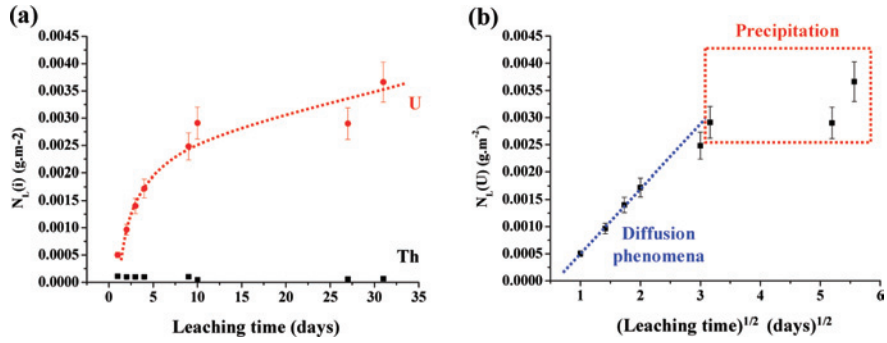

Figure 2. Evolution of N_L(Th) (■) and N_L(U) (●) during the dissolution of $Ca_{0.5}Th_{0.4}U_{0.1}PO_4$ sample leached in 10^{-1}M HNO_3 at 90 °C (a) and associated variation of N_L(U) vs the square root of time (b).

3.2. Experimental Study of the Dissolution of Monazite/Brabantite Solid Solutions. 3.2.1. Static Conditions. Samples of monazite/brabantite (monazite/cheralite) solid solutions were leached in static conditions for several pH values and temperatures. The evolution of N_L(U) and N_L(Th) are reported for leaching tests on $Ca_{0.5}Th_{0.4}U_{0.1}PO_4$ in 10^{-1}M HNO_3 at 90 °C (Figure 2a). The dissolution is clearly characterized by the rapid precipitation of thorium while uranium is released in the solution. As it was reported for Th-britholites, the formation of $Ca_xNd_{1-2x}Th_xPO_4 \cdot {}^1/_2\ H_2O$ rhabdophane needle-like crystals was evidence in such experimental conditions onto the surface of the leached pellets.[76] Moreover, as it was observed during the dissolution of other phosphate-based radwaste matrices,[78] the precipitation starts with the formation of gelatinous phase at the solid-solution interface followed by the nucleation of small crystals. Both amorphous and crystalline neoformed Ca,Th-bearing phases are expected to induce diffusion phenomena that can modify the release of the other elements. Finally, as already mentioned in the previous section, such reactions are usually increasing with the leaching time.[69,76,78] On this basis, the evolution of N_L(U) clearly evidences two tendencies: during the first 5 days, the R_L(U) values ranges from 10^{-5} to 10^{-4} g·m^{-2}·day^{-1} and are in good agreement with that reported in the literature.[22,64,65,76] Moreover, they appear to be on the same order of magnitude as that reported for β-TUPD or β-TUPD/monazite samples[13,69] and are low compared to that determined for britholites. A decrease of the normalized leaching rate of uranium is then observed after 5 days of dissolution. The linear variation of N_L(U) versus the square root of time (Figure 2b) accounts for the diffusion of uranium through the neoformed layer formed consequently to the saturation of the leachate. For longer leaching times, a plateau is associated to the precipitation of uranium in neoformed phases.

The behavior of monazite/brabantite solid solutions loaded with thorium and lanthanides, showed similar tendency but is associated to normalized dissolution rates slower (9.4×10^{-7} g·m^{-2}·day^{-1} ≤ R_L(La,Eu) ≤ 1.7×10^{-6} g·m^{-2}·day^{-1}) than that obtained for pure brabantite (cheralite) samples (Table 2). Moreover, as reported for britholites, the presence of tetravalent uranium slightly degrades the chemical durability of the samples due to its tendency to oxidize at the solid−liquid interface during the dissolution process.

Table 2. Normalized Dissolution Rates R_L (g·m^{-2}·day^{-1}) Determined during the Dissolution of $La_{0.4}Eu_{0.1}Ca_{0.25}Th_{0.25}PO_4$ Samples in Static Conditions at 90°C in 10^{-1}M HNO_3[a]

	$La_{0.4}Eu_{0.1}Ca_{0.25}Th_{0.25}PO_4$	
leaching time	<7 days	>7 days
La	$(1.7 \pm 0.2)\ 10^{-6}$	$(1.9 \pm 0.2)\ 10^{-7}$
Eu	$(4.3 \pm 0.4)\ 10^{-6}$	$(9.4 \pm 0.9)\ 10^{-6}$

[a] R_L(Th) values were not determined since the thorium concentrations were found to be below the detection limit of the used method.

3.2.2. Dynamic Conditions. To avoid (or delay) the saturation phenomena observed, some experiments were also undertaken in dynamic conditions on monazite/brabantite (monazite/cheralite) solid solutions. The evolution of the normalized leachings, N_L(U), obtained when leaching $Ca_{0.5}Th_{0.5-x}U_xPO_4$ samples in dynamic conditions for several media and temperatures are plotted in Figure 3, and the associated normalized dissolution rates are gathered in Table 3. These values show the same tendency as when using static conditions; the R_L(U) obtained when leaching the samples in 10^{-1}M HNO_3 at 90 °C increases from $(2.2 \pm 0.2)\ 10^{-5}$ g·m^{-2}·day^{-1} for $Ca_{0.5}Th_{0.5}PO_4$ to $(4.6 \pm 0.5)\ 10^{-3}$ g·m^{-2}·day^{-1} for $Ca_{0.5}Th_{0.2}U_{0.3}PO_4$, confirming the significant degradation of the chemical durability of the samples when loading the materials with tetravalent uranium, probably due to its tendency to be oxidized in the uranyl form at the solid/liquid interface. Even for high renewals of the leachate, a decrease of the R_L(U) values is often observed after 2−4 days of dissolution, consequent to the precipitation of thorium enriched neoformed phases. The same behavior is observed for monazite/brabantite solid solutions.

The direct comparison of britholites and monazite/brabantite (monazite/cheralite) solid solutions shows that the chemical durability of the latter is far better for all the leaching conditions examined. Indeed, the normalized dissolution rates values are strongly different even if the dissolution is incongruent, whatever the solid considered, with the probable precipitation of thorium into highly insoluble neoformed phases then diffusion of uranium through the passivation layer. Depending on the nature of the samples and the leaching conditions (medium, temperature, etc.), the normalized dissolution rates ratio R_L(britholite)/R_L(monazite/brabantite) is always found to be between 10^3 and 10^6. Because both matrices contain significant

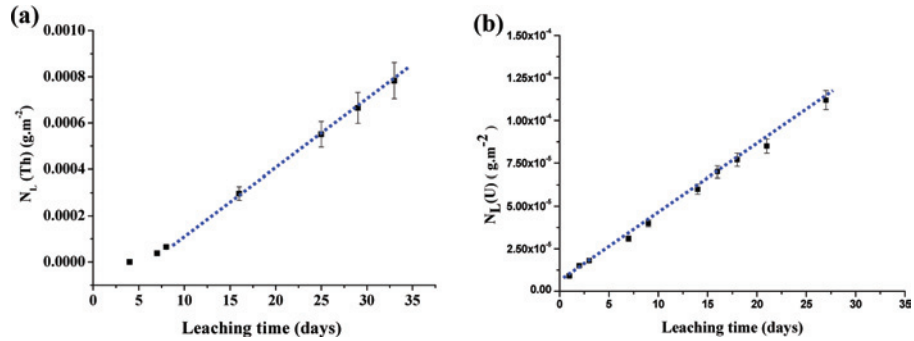

Figure 3. Evolution of N_L(Th) or N_L(U) during the dissolution of $Ca_{0.5}Th_{0.5}PO_4$ at 90 °C (a) and of $Ca_{0.5}Th_{0.4}U_{0.1}PO_4$ at 70 °C (b) in 10^{-1}M HNO_3.

Table 3. Normalized Dissolution Rates Obtained during the Dissolution of (Ca,Th,U)-Brabantites (Cheralites) and (La,Ca,Th,U)-Monazite/Brabantite (Monazite/Cheralite) Solid Solutions in 10^{-1}M HNO_3

	t (days)	T (°C)	R_L(An) (g·m^{-2}·day^{-1})*
$Ca_{0.5}Th_{0.5}PO_4$		90	(2.2 ± 0.2) 10^{-5}
$Ca_{0.5}Th_{0.4}U_{0.1}PO_4$		70	(9.7 ± 0.8) 10^{-5}
$Ca_{0.5}Th_{0.2}U_{0.3}PO_4$	<2	70	(4.6 ± 0.5) 10^{-3}
	>2		(1.4 ± 0.1) 10^{-3}
$Ca_{0.5}Th_{0.1}U_{0.4}PO_4$	<2	70	(2.4 ± 0.2) 10^{-3}
	>2		(1.8 ± 0.2) 10^{-3}
$La_{0.50}Ca_{0.25}Th_{0.15}U_{0.10}PO_4$	<8	70	(1.7 ± 0.2) 10^{-3}
	>8		(7.9 ± 0.8) 10^{-4}

* Normalized dissolution rates determined from the release of thorium for Th-brabantite and that of uranium for (Ca,Th,U)-brabantites and (La,Ca,Th,U)-monazite/brabantite solid solutions.

amounts of calcium, which is usually considered as a more leachable element compared to lanthanides or actinides, their behaviors should be comparable. For this reason, these different behaviors during the dissolution processes were examined in the field of structural differences. Indeed, britholites present an open structure based on huge canals, which could bring an explanation for their lower chemical durability. On the contrary, monazite/brabantite (monazite/cheralite) solid solutions exhibit a very compact structure, which is probably responsible of their high resistance to aqueous corrosion. To validate this assumption, the cohesive energy of the calcium atoms was determined for both solids using a periodic DFT approach.

3.3. Periodic DFT Results. 3.3.1. Study on (Nd,Th)-Britholites. The hexagonal unit cell used for all the calculations on (Nd,Th)-britholites was composed of four elementary cells, with the general composition $Ca_{36}Nd_2Th_2(PO_4)_{20}(SiO_4)_4F_8$. According to literature,[51,80] three-quarters of the promotor atoms (thorium and neodymium) occupy the calcium site (II) in the structure, corresponding to 7-fold coordinated atoms and belonging to a calcium channel occupied by fluorine ions (Figure 4). The remaining one-quarter atoms are located in site (I) and are 9-fold coordinated (Figure 4).

Two distinct structures were built in order to take into account different promotor distributions in the bulk (Table 4). Particularly, the structure (II) displays a slightly lower dispersion of the promotor atoms in the bulk and therefore allows one to study the effect of the presence of more than one promotor atom in the neighborhood of the calcium atom.

For both structures, the lattice vectors and angles obtained after the bulk relaxation (Table 5) are in good agreement with the values reported in the literature.[16,17] Those results

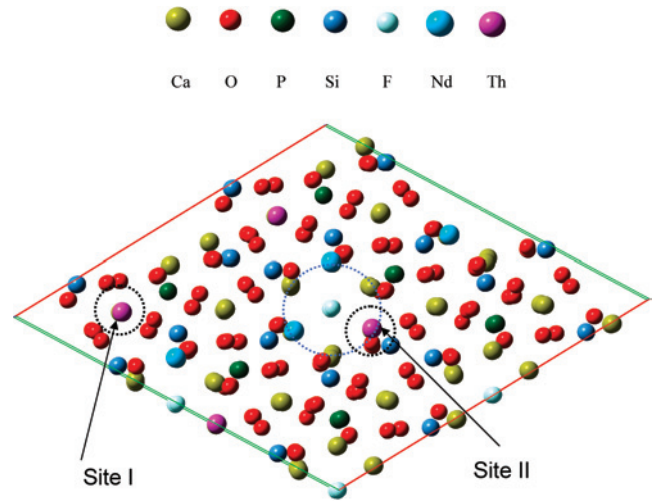

Figure 4. The (001) view of the promoted britholite structure. Location of the two kinds of sites (black dot lines). A Blue dot line represents the open channel.

Table 4. Promotor Atoms Distribution in Sites (I) and (II) for Structures (I) and (II).

	structure (I)	structure (II)
site (I)	Th	Nd
site (II)	Th, Nd, Nd	Nd, Th, Th

Table 5. Calculated Unit-cell Parameters for Both Promoted (Nd,Th)-Britholite Structures and Associated Experimental Data[17]

	experimental	structure (I)	structure (II)
a (Å)	9.408(2)	9.506	9.502
b (Å)	9.408(2)	9.548	9.549
c (Å)	6.910(1)	6.908	6.921
α (°)	90	90.07	90.03
β (°)	90	89.96	89.98
γ (°)	120	119.92	120.08

led us to consider the two promoted structures presented in Figure 5 to calculate the cohesive energies of calcium atom in the (Th,Nd)-britholite configurations.

To study the properties of calcium vacancies, one neutral atom of the super cell was removed as usually performed.[81] The cohesive energy of the calcium atom *(E)* was thus calculated using eq 6:

$$E = E(\text{system\_}b) + E(\text{Ca}) - E(\text{system\_}a) \qquad (6)$$

where the E values are directly calculated using the VASP code as described above, E(system_b) corresponds to the energy of the relaxed vacancy system, E(Ca) is the energy of one calcium atom, and E(system_a) is the energy of the relaxed promoted solid without any vacancy. To determine

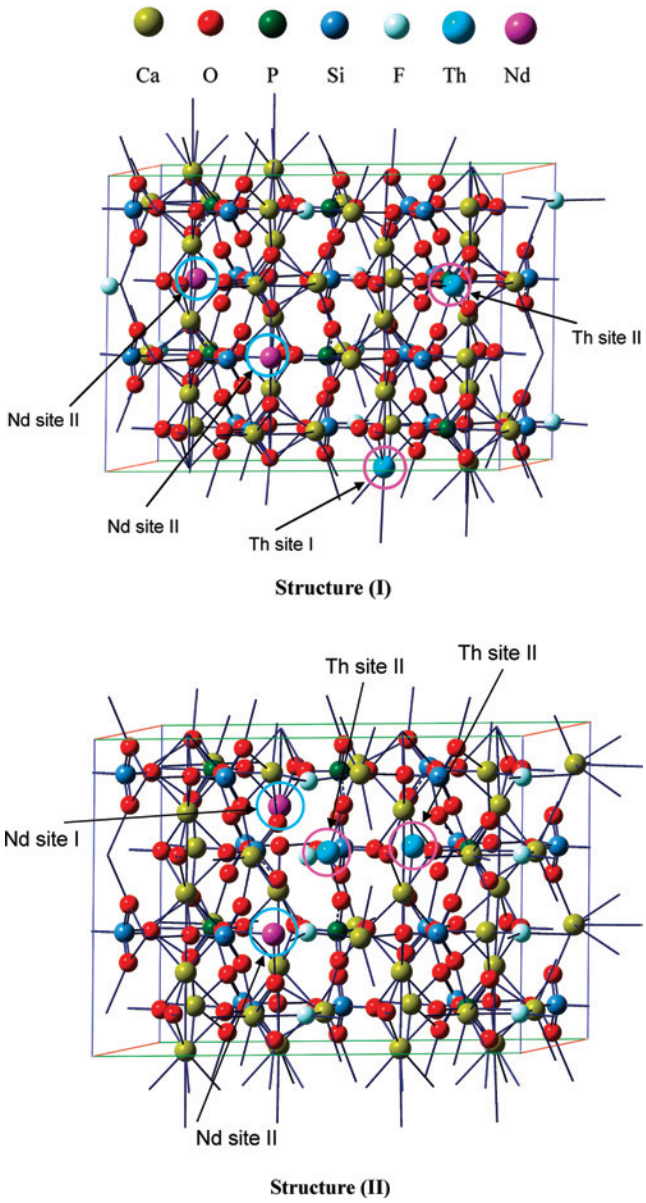

Figure 5. Representation of structure (I) and (II) considered for (Nd,Th)-Britholite. Thorium promotor atoms are surrounded in purple and neodymium promotor atoms are surrounded in blue. The promotor site is also indicated.

the energy *E*(Ca), calculations were performed using the Ca α-phase bulk parameters.[82] This phase corresponds to the most stable allotropic form of calcium for normal temperature and pressure conditions.

The main characteristics of the four investigated vacancy structures are displayed in Table 6. For both structures, the calculated cohesive energies of calcium range between 8.42 and 10.02 eV.

The nature of the sites (I) or (II) significantly influences the cohesive energy of calcium. Indeed, as it can be seen from Table 6, the (c), (d), and (h) configurations, related to site (II), led to higher energies than the (a) and (b)

Table 6. Calcium Sites and Nature of the Closer Promotor Atom (Neodymium and/or Thorium), Cohesive Energy (eV) of Calcium Atom, and Distance between the Promotor(s) and the Calcium Atom (Å)

configuration	promotor/ Ca site	cohesive energy (eV)	*d*(Ca−promotor) (Å)
Structure (I)			
(a)	Th - Site (I)	9.08	3.52
(b)	Nd - Site (I)	9.51	3.99
(c)	Nd - Site (II)	9.92	3.91
(d)	Th - Site (II)	9.61	3.91
Structure (II)			
(e)	(Nd,Th) - Site (I)	8.37	3.69; 4.37
(f)	(Th,Th) - Site (I)	8.42	3.84; 4.01
(g)	(Th,Nd) - Site (II)	9.10	4.21; 4.28
(h)	Th - Site (II)	10.02	5.77

configurations associated with site (I). This could be explained by the formation of strong Ca−F bond in site (II), which does not exist in site (I). On the other side, the presence of thorium atoms located in the vicinity of the calcium atom leads to the decrease the cohesive energy compared to neodymium atom, whatever the site considered. The comparison of configurations (a) and (b) (site (I)), on the one hand, and (c) and (d) (site (II)), on the other hand, clearly supports this evidence. It is also observed that the number of promotors clearly influences the cohesive energy of calcium. Indeed, this latter decreases when the promotor number surrounding the calcium atom increases from one to two. Finally, the more the promotor is close to the calcium atom, the lower is the cohesive energy of calcium atom (see the comparison between configurations (d) and (h)). From this study, the cohesive energy of calcium in (Nd,Th)-britholites is thus influenced by four parameters: the nature of the calcium site; the nature of promotor atoms; the number of promotor atoms; and the distance between the promotor(s) and calcium.

3.3.2. Study on (La,Ca,Th)-Monazite/Brabantite Solid-solutions. The unit cell considered for periodic calculations is built with two primitive unit cells of (La,Ca,Th)-monazite/brabantite (monazite/cheralite). The unit cell therefore contains eight $LaPO_4$ entities (crystallographic parameters are displayed from literature[50]) where two lanthanum atoms are substituted by one calcium and one thorium atom.

Two different structures were built to take into account the promotor dispersion through the bulk. In the first one (Figure 6a), calcium and thorium atoms are systematically separated by phosphate groups whatever the direction considered, leading to a minimal calcium-to-thorium distance of 6.62 Å. It is not the case in the second structure (Figure 4b), where promotor atoms are closer and separated by a minimal distance of 4.10 Å. The promotors dispersion into the bulk is, therefore, lower compared to structure (I).

As for (Nd,Th)-britholite samples, the lattice parameters calculated for both structures clearly show a good agreement with the experimental crystallographic data (Table 7).

Using eq 6, the cohesive energies of calcium were calculated to 10.78 and 10.74 eV, respectively, in structure (I) and (II) (Figure 6). In these conditions, thorium atoms do not induce a significant modification of the cohesive energy of calcium, whatever their location in the bulk. Consequently, it can be questioned if thorium atoms really generate an electronic effect on the cohesive energy of calcium. Hence, it appears interesting

(80) Meis, C. *J. Nucl. Mater.* **2001**, *289*, 167–176.
(81) Grau-Respo, R.; de P.R. Moreira, I.; Illas, F.; de Leeuw, N. H.; Catlow, C. R. A. *J. Mater. Chem.* **2006**, *16*, 1943–1949.
(82) *EnvironmentalChemistry.com*; Element Calcium - Ca http://Environmentalchemistry.com/yogi/periodic/Ca.html

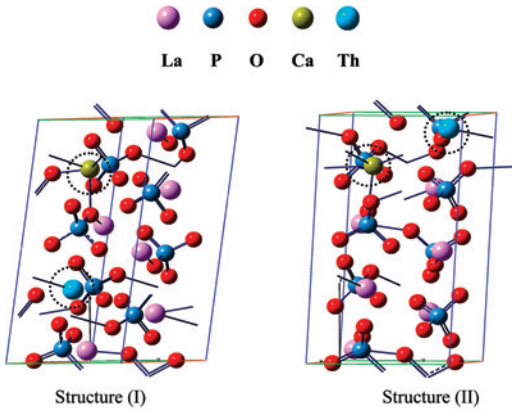

Figure 6. Promoted (La,Ca,Th)-monazite/brabantite solid-solution structure (I) and structure (II), with a lower dispersion of the promotor for structure (II). Promotor calcium and thorium atoms are surrounding by black dash lines.

Table 7. Calculated Parameters for the Promoted (La,Ca,Th)-monazite/brabantite Structures (I) and (II) Considered and Associated Experimental Parameters[50]

	experimental	structure (I)	structure (II)
a (Å)	6.825(1)	6.865	6.859
b (Å)	7.057(1)	7.094	7.088
c (Å)	6.482(1)	6.555	6.551
α (°)	90	90.34	90.23
β (°)	103.21	103.62	103.51
γ (°)	90	89.95	89.90

to calculate the energy to remove a calcium atom when no thorium atom subsists in the structure. In this case, a cohesive energy of 11.00 eV is calculated. This plainly indicates that thorium atoms provoke a decrease of the vacancy creation energy, although the effect is rather weak for this kind of materials.

Periodic DFT calculations undertaken in both materials clearly put forward the stronger promotor effect of thorium and neodymium onto the calcium atoms removal into (Nd,Th)-britholite. Conversely, the influence of thorium promotor appears significantly smaller in the structure of monazite/brabantite solid solutions. Furthermore, the difference observed between the cohesive energies in (La,Ca,Th)-monazite/brabantite solid solutions and in (Nd,Th)-britholite (ranging from 0.72 and 2.41 eV) indicates that the lower chemical durability of britholites evidenced during the leaching experiments could be associated to the lower energy required to remove calcium atoms in (Nd,Th)-britholites compared to (La,Ca,Th)-monazite/brabantite solid solutions. Moreover, calcium atoms located in site (I) are even easier to remove compared to that present in site (II). This may be explained by the formation of strong Ca (site II) −F bonds in the (Nd,Th)-britholite channel. This point appears of great importance since it can be correlated to the experimental data. Indeed, for the major part of the leaching tests examined in acidic media on (Nd,Th)-britholite samples, the incongruent dissolution was associated to the preferential release of calcium in the leachate compared to the other cations, which can be correlated to the relative "resistance" of site (II) compared to site (I), in which the incorporation of calcium by other cations is more important. Additionally, the ability to remove a calcium atom in (Nd,Th)-britholite also depends on the promotor to calcium distance as well as on the number of promotor atoms close to calcium atoms. Calculations displayed a more-pronounced promotor effect of thorium atoms compared to neodymium ones. On the contrary, the distance between the promotor and calcium induces only small effects on the formation of vacancy for (La,Ca,Th)-monazite/brabantite solid solutions. Finally, the influence of promotor atoms is surely partially responsible of the sensitivity of (Nd,Th)-britholites during aqueous alteration. Conversely, the small influence of this parameter for (La,Ca,Th)-monazite/brabantite solid solutions associated to higher values of energy of cohesion could explain the higher resistance of this kind of structure during alteration processes. This latter point must be also considered in the light of the geochemical observations already reported for this kind of materials that suggest that the chemical flexibility and the high resistance of the monazite structure to aqueous alteration and to radiation damage is probably due to the distorded and flexible cationic environment in such structure.[1,23]

4. Conclusion

The direct comparison of (Nd,An)-britholites and (La,Ca,An)-monazite/brabantites (monazite/cheralite) samples containing significant amounts of thorium and/or uranium reveals the stronger resistance of the latter compound during leaching tests. Indeed, even though the formation of strongly insoluble neoformed phases are highly efficient for both kinds of materials to control and then delay the release of elements such as thorium or uranium in the leachate when saturation processes are reached, the normalized dissolution rates determined for (Nd,An)-britholite samples are found to be 3−6 orders of magnitude higher than that obtained for (La,Ca,An)-monazite/brabantite solid solutions. This difference was examined in the light of periodic DFT calculations, especially when considering the promotor effect in both matrices. From this study, it appeared that this effect is significant in the (Nd,Th)-britholite structure and is significantly lower in that of (La,Ca,An)-monazite/brabantite (monazite/cheralite) solid solutions. Furthermore, an important difference is also observed between the cohesive energy of calcium in (La,Ca,Th)-monazite/brabantite and (Nd,Th)-britholite samples. In such conditions, the calcium atoms should be more easily released when leaching (Nd,Th)-britholite samples (especially calcium atoms present in site (I)), which appears in very good agreement with the data acquired during the leaching tests. Additionally, the ability to remove a calcium atom in (Nd,Th)-britholite also depends on the number and on the nature of the promotors, as well as the promotor to calcium distance, which is not the case for (La,Ca,Th)-monazite/brabantite samples.

Acknowledgment. This work was financially supported by the French research group NOMADE (NOuveaux MAtériaux pour les DEchets, GDR 2023 CNRS/CEA/AREVA/EDF/French Universities). The authors would like to thank Dr. J. Aupiais (CEA/Bruyères le Châtel, France) for his precious scientific and material support during the ICP-AES and KPA experiments. A generous allotment of CPU time on GRIF (http://www.grif.fr) is also gratefully acknowledged.

IC801169D